

Experimental Test of Theories of the Detection Mechanism in a Nanowire Superconducting Single Photon Detector

J. J. Renema,^{1,*} R. Gaudio,² Q. Wang,¹ Z. Zhou,² A. Gaggero,³ F. Mattioli,³ R. Leoni,³ D. Sahin,² M. J. A. de Dood,¹ A. Fiore,² and M. P. van Exter¹

¹*Leiden Institute of Physics, Leiden University, Niels Bohrweg 2, 2333 CA Leiden, Netherlands*

²*COBRA Research Institute, Eindhoven University of Technology, Post Office Box 513, 5600 MB Eindhoven, Netherlands*

³*Istituto di Fotonica e Nanotecnologie (IFN), CNR, via Cineto Romano 42, 00156 Roma, Italy*

(Received 12 August 2013; revised manuscript received 9 December 2013; published 21 March 2014)

We report an experimental test of the photodetection mechanism in a nanowire superconducting single photon detector. Detector tomography allows us to explore the 0.8–8 eV energy range via multiphoton excitations. High accuracy results enable a detailed comparison of the experimental data with theories for the mechanism of photon detection. We show that the temperature dependence of the efficiency of the superconducting single photon detector is determined not by the critical current but by the current associated with vortex unbinding. We find that both quasiparticle diffusion and vortices play a role in the detection event.

DOI: 10.1103/PhysRevLett.112.117604

PACS numbers: 79.20.Ws, 03.65.Wj, 85.25.Oj

Nanowire superconducting single photon detectors (SSPDs or SNSPDs) [1,2] are currently the most promising detection systems in the infrared, achieving detection efficiencies of up to 93% at 1550 nm [3]. Despite these technological advances, the fundamentals of the working principle of these detectors are poorly understood and under active investigation, both theoretically [4–11] and experimentally [12–22].

A typical SSPD consists of a few nm thin film of a superconducting material such as NbN or WSi, nanofabricated into a meandering wire geometry. When biased sufficiently close to the critical current of the superconductor, the energy of one or several photons can be enough to trigger a local transition to the resistive state, resulting in a detection event. The energy of the absorbed photon is distributed through an avalanchelike process, creating a nonequilibrium population of quasiparticles. This quasiparticle population then disrupts the supercurrent flow, resulting eventually in a detection event.

In this Letter, we address the nature of this disruption, which lies at the heart of the photodetection mechanism in SSPDs. At present, there are three important open questions. First, it is unknown whether the detection event occurs when the energy of the incident photon causes a cylindrical volume inside the wire to transition to the normal state [see Fig. 1(a)] [1], or whether it is enough for the superconductivity to be weakened but not destroyed by the depletion of Cooper pairs over a more extended region [see Fig. 1(b)] [4].

The second open question is whether magnetic vortices play any role in the detection mechanism. There are two varieties of vortex-based models. The first is an extension of the normal-core model, where, a vortex-antivortex pair forms at the point where the photon is absorbed [Fig. 1(c)] [5]. In the second, the weakening of superconductivity

lowers the energy barrier for either a vortex crossing [6,23] or a vortex-antivortex pair crossing [Fig. 1(d)].

The last open question pertains to the temperature dependence of the photoresponse of SSPDs. Intuitively, one would expect the SSPD to be less efficient at lower temperatures, as the detector works by breaking superconductivity and the energy gap of a superconductor decreases with increasing temperature. However, the opposite effect is consistently observed [12]. Apart from a study of the temperature dependence of the diffusion constant [8], no real headway has been made in this problem.

Our experimental results provide answers to all three questions. In short, we show that both quasiparticle

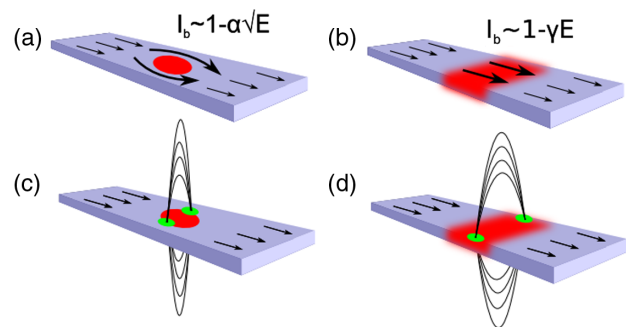


FIG. 1 (color online). Sketches of the four main detection models. (a) In the normal-core hot spot model, the photon energy creates a normal domain inside the superconductor, which the current has to bypass. (b) In the diffusion-based hot spot model, the quasiparticles diffuse outward from the point of absorption, creating a band of depleted superconductivity. (c) In the vortex-nucleation model, a vortex-antivortex pair is formed in the hot spot. (d) In the vortex crossing model, either a vortex or a vortex-antivortex pair (pictured) uses an area of weakened superconductivity to cross the wire and annihilate. Picture is not to scale.

diffusion and vortices play a role in the detection event. We achieve the first result by measuring the functional dependence between the bias current and photon energy required for a constant detection probability. The observed linear functional dependence is incompatible with the original hot spot model and demonstrates the importance of diffusion. Our evidence for the role of vortices lies in the observation of a reference current which sets the efficiency of the detection mechanism and which is unequal to the critical current and also has a different temperature dependence. At the temperature where the reference current crosses the critical current, the efficiency of the detector degrades. We find that the temperature dependence of the reference current matches that of the current at which vortices can unbind from the sides of the detector.

Experiment.—We perform the majority of our experiments on a 220 nm wide bow-tie nanodetector [24]. The detector is patterned from a 5 nm thick NbN film deposited on a GaAs substrate. The detector is fabricated by electron beam lithography and reactive ion etching. Photodetection takes place in the narrow ($w_0 = 220$ nm wide) part of the bow tie, where the current density is highest.

We significantly extend the energy range over which we probe the detector compared to previous experiments [12,13]. The energy range in our experiment runs from 0.75 to 8.26 eV, corresponding to $\lambda_{\text{eff}} = 1650\text{--}130$ nm. We achieve this extension of the energy range by using multiphoton excitations, which are resolved by detector tomography [25–28]. Detector tomography is a method of quantum detector characterization that relies on illuminating a photon detector with a series of known quantum states and observing the photoresponse. In our case, we use coherent states from a broadband supercontinuum laser, which was spectrally filtered [29]. These states have known photon number distributions which are set by the classical laser intensity, which can be easily varied. From this, we determine the response to each individual number of photons, i.e., the Fock-basis response [30]. The strength of our modified detector tomography is that it allows us to separate the incoupling and absorption efficiency η , i.e., the probability to absorb a photon, from the internal detection probability p_n , i.e., the probability of a detection event after the absorption of n photons. A detailed description of our method can be found in [28] [31].

Results and discussion.—Figure 2 shows the measured combinations of bias current I_b and photon energy $E = n(hc/\lambda)$ for which the detection probability equals 1% after absorption of n photons. We achieved this result by performing detector tomography at twelve different wavelengths, and finding the current at which n photons (indicated in the legend) have the required probability to cause a detection event.

To validate our experimental method of using multiphoton excitations to probe the detection mechanism, we measured at wavelengths that are harmonics

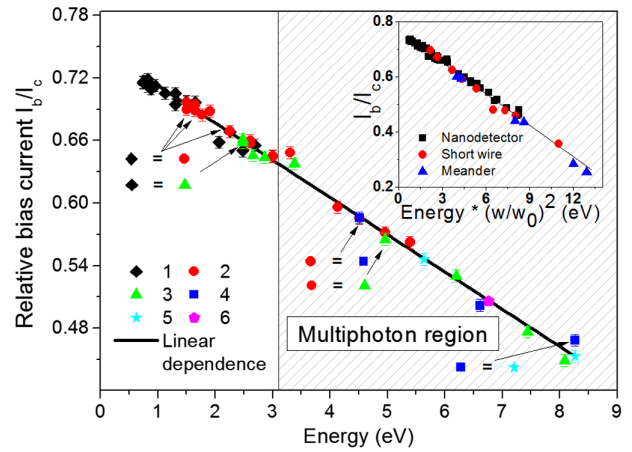


FIG. 2 (color online). Quantum tomography of superconducting single photon detectors. We plot the bias current required to obtain a 1% probability of a given detection event, as a function of the overall energy of the multiphoton excitation. The points are the experimental data: their shape and color indicates the number of photons associated with each excitation. The arrows indicate those points where two photon energies coincide. The line shows a linear interchange between bias current and excitation energy. The shaded area indicates the regime that is only accessible with multiphoton excitations. Inset: comparison of a nanodetector, a short (400 nm) wire, and a meander. We find that the response of the wire and meander coincides with that of the nanodetector, taking into account the difference in width between these three detectors by normalization to the width w_0 of the nanodetector.

(e.g., $\lambda = 1500$ and $\lambda = 500$ nm). We consistently find that the result of these measurements overlap over the entire measurement range, and have indicated these points with arrows in Fig. 2. This demonstrates that, irrespective of which detection model is correct, the observed probabilities p_n depend only on bias current and overall excitation energy $E = n(hc/\lambda)$. This is an independent justification of the use of multiphoton excitations to test the detection mechanism.

We can parametrize our complete set of measurements by the expression $I = I_0 - \gamma E$, where I is the observed current required to achieve $p_n = 0.01$, and E is the overall energy of the excitation. The slope γ describes the interchange between bias current and photon energy. By extrapolating to $E = 0$, we find a current I_0 that is unequal to the critical current I_c and which we name the *reference current*, since it functions as the baseline from which the detector response may be determined. At $T = 3.2$ K, we find $I_0/I_c = 0.75$. This experimental result does not change significantly with the choice of threshold criterion. The linear relation persists; a 10% threshold criterion gives $I_0/I_c = 0.79$.

In the regime $I_0 < I_b < I_c$, all multiphoton detection probabilities p_n of the detector are constant. However, we find that the linear efficiency η increases in this regime. We attribute this to the fact that in our bow-tie structure, a larger area of the detector is above I_0 . It is known that for efficient meander detectors, there is a plateau region where the

detector response is constant with current [3]. We note that dark counts occur in our system when $I_b \approx I_c$. Around I_0 , we do not measure any dark counts in a 30 s interval. This demonstrates—surprisingly enough—that extrapolation to $E = 0$ does not yield the dark count rate.

Figure 2 demonstrates that the relation between bias current and photon energy required to have a constant detection probability is linear, over 1 order of magnitude in energy. This result demonstrates that the detection process is not associated with any normal-state region that is formed in the SSPD. For a normal-core model, the energy dependence would be quadratic, as can be seen from a simple geometric argument that relates the lateral size of the obstruction made by the normal core to the photon energy [32]. For a model in which there is no normal state, the current carrying capacity of the wire is linearly dependent on the number of remaining cooper pairs and therefore on the photon energy.

We will now demonstrate that we can use our nanodetector as a model system of an SSPD. We compare our results with those on a $w = 150$ nm wide, 400 nm long, wire and a conventional $w = 100$ nm meander detector [33]. The inset of Fig. 2 shows a comparison of our three detectors. We take into account the width w of the detector by normalizing the energy scales to the width of the nanodetector, which enters through both the critical current and through the intrinsic $1/w$ scaling of the detection mechanism [32]. For our nanodetector, wire, and meander, the results superimpose. This demonstrates that our nanodetector functions as a model of an SSPD.

Figure 3 shows the experimental observations at $\lambda = 600$ nm, for the $n = 1$ to $n = 4$ photon regime. By restricting ourselves to one wavelength, we can improve the accuracy of our experiment by removing all systematic errors associated with changing wavelength. These data are representative of the accuracy of our experimental runs at other wavelengths. We fit a general expression $I = I_0 + \gamma E^\alpha$ to this selection. As noted above, we expect to find $\alpha = 0.5$ for the normal-core hot spot model and $\alpha = 1$ for a diffusion-type model. For the vortex-based models, the expressions are more complex, but can be approximated by $\alpha = 0.5$ and $\alpha = 0.75$ for the vortex nucleation and vortex crossing models, respectively [5–7,13] [34]. We experimentally find $\alpha = 1.00 \pm 0.06$, indicating good agreement with the diffusion model. We note, however, that since the most straightforward variant of the diffusion model predicts $I_0 = I_c$, this cannot be the whole story. We must therefore look for additional effects to explain the detection mechanism in SSPDs.

In Fig. 4, we show the temperature dependence of the observed reference current I_0 , measured on the nanodetector, normalized to the experimental critical current. We obtain this plot by performing an experiment as shown in Fig. 2 at various temperatures. We experimentally find that only the current scale I_0 is temperature dependent; the

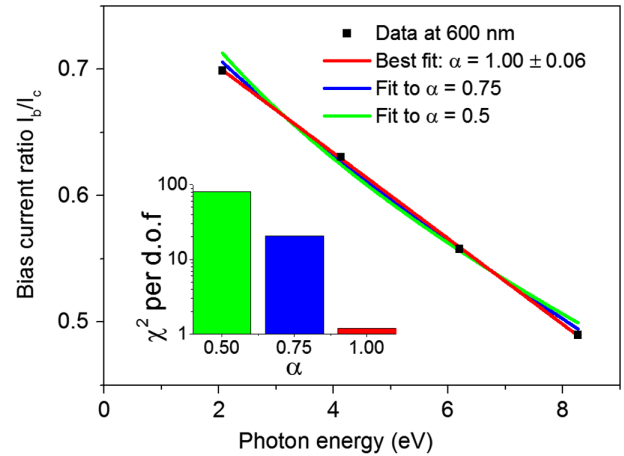


FIG. 3 (color online). Experimental results on quantum detector tomography at $\lambda = 600$ nm. We show a single run of the experiment from Fig. 2. To these data, which are free of the systematic error associated with changing wavelength, we fit a general expression $I = I_0 - \gamma E^\alpha$, where the value of α determines which model we are in. We find $\alpha = 1.00 \pm 0.06$, indicating good agreement with the linear (diffusion) model. We plot fits to $\alpha = 0.5$ and $\alpha = 0.75$ for comparison. Inset: χ^2 of the three fits. We find that scenarios with a nonlinear energy-current relation are strongly inconsistent with our experimental data.

incoupling efficiency η and energy-current slope γ are independent of temperature. The temperature dependence of I_0 therefore completely describes the temperature behavior of the device. I_c follows the Ginzburg-Landau

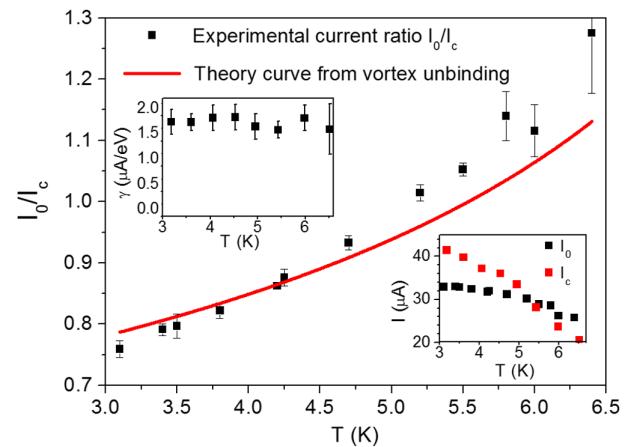


FIG. 4 (color online). Temperature dependence of the fundamental current I_0 in the nanodetector, relative to the critical current. The red curve shows the temperature dependence of the ratio of the current associated with the vortex energy barrier (the barrier that a vortex has to overcome to enter the device), and the Ginzburg Landau critical current [6,7]. Top inset: temperature dependence of the energy-current interchange ratio γ . This parameter, and the overall linear efficiency η are both temperature independent to within our experimental accuracy. Bottom inset: Temperature dependence of I_0 and I_c , separately. I_c follows the temperature dependence of the GL depairing current.

temperature dependence, which is consistent with the result found on Nb bridges [35]. The key result from Fig. 4 is that the temperature dependence of the reference current is different from that of the critical current.

We first discuss the implications of our results for the practical use of SSPDs. Around $T = 5.5$ K, we find $I_0 \approx I_c$. This means that above this temperature, there are energies for which the detector no longer operates fully as a single-photon detector. This observation explains the strong reduction in performance that detectors experience around this temperature. Note that with the usual semi-classical characterization, one can always find a regime where measured count rates are linear with input power by going to sufficiently low power, even at $p_1 \ll 1$. The transition from single to multiphoton detection that we have found can therefore only be observed by the use of detector tomography.

Our experimental I_c follows the Ginzburg-Landau $I_c(T) = I_c(0)(1 - T/T_c)^{3/2}$ dependence of the depairing current, i.e., the current at which the Cooper pair binding energy is reduced to zero. The reference current I_0 has a different temperature dependence. As vortices are the other major effect in type-II superconductors, it is natural to consider whether the observed current scale pertains to vortices. Vortices are affected by the Lorentz force, and an unpinned vortex would be driven across the width of the strip by the bias current. We must therefore consider dynamic vortex scenarios.

Based on the above considerations, we compare the reference current to the current scale that governs the height of the energy barrier for a vortex crossing [6,7]. The ratio I_0/I_c contains an explicit temperature dependence through the superconducting coherence length $\xi(T) \sim (1 - T/T_c)^{-0.5}$ ($T_c = 9.6$ K). In Fig. 4, we plot this temperature dependence. The existence of an alternate current $I_0 \neq I_c$ in SSPDs, and the observation that the temperature dependence of this current follows the temperature dependence of the binding energy of a vortex is evidence for the fact that the detection mechanism is vortex based and that the temperature dependence is set by this energy.

SSPDs can also be used in the keV regime, either for detecting x-ray photons [36] or for detecting ions. The experiment by Suzuki *et al.* [14] on ion detection in 800 nm wide, 10 nm thick, detectors has clearly demonstrated that the normal-core hot spot model is correct in the keV range. This is understandable, as a single injection of a large amount of energy will be enough to break all the Cooper pairs at a single position along the wire, leading to a normal-core scenario. There must therefore be a typical energy where the diffusion-based scenario gives way to a normal-core scenario. By fitting only low-energy events and extrapolation to high energies, we can check whether all our results are described by a single model. We find that this is the case, and therefore conclude that this transition occurs at an energy higher than 8 eV, for our system.

The overall conclusions which may be drawn from our results are that both vortices and diffusion play a role in the detection event. Returning to Fig. 1, we may therefore conclude that scenario (d) is the one that corresponds closest to reality. We note, however, that the particular vortex crossing model proposed by Bulaevskii *et al.* has a current-energy dependence that does not correspond to our experimental observations. This point was addressed in a recent article by Engel and Schilling [37], which combines diffusion and vortex crossing in a numerical simulation. However, both the numerical simulation and the theoretical work predict $I_0 = I_c$ for the limit $T \rightarrow 0$. More theoretical work is needed to explain our results.

Conclusion.—We have experimentally demonstrated that the dependence between the excitation energy and bias current required to produce a detection event in a superconducting single photon detector is linear. The exact linear dependence in the experiment is consistent with a detection model that relies on the diffusion of quasiparticles produced by the initial excitation. Other models produce behavior that deviates significantly from the linear dependence.

We find a current scale which characterizes the response of the detector which is unequal to the critical current of the device. When the temperature is increased, we find that the observed current scale exceeds the critical current at the same temperature where the SSPD response degrades. We observe no temperature dependence in the other observed parameters, which together provide a complete description of the detector. We therefore conclude that we have localized the problem of temperature dependence of SSPDs to a single current scale. The observed temperature dependence matches reasonably well with a theory describing the crossing of a single vortex. From our results, it is clear that at optical frequencies, quasiparticle diffusion and vortex unbinding are the two main ingredients in any model of SSPD behavior.

We thank S. Jahanmirinejad, G. Goltsman, D. Y. Vodolazov, A. Engel, P. Kes, J. Aarts, R. J. Rengelink, I. Komen, E. Driessen and T. Klapwijk for useful discussions, D. Boltje for technical assistance and F. Schenkel for assistance with the experimental apparatus. This work is part of the research programme of the Foundation for Fundamental Research on Matter (FOM), which is financially supported by the Netherlands Organisation for Scientific Research (NWO) and is also supported by NanoNextNL, a micro- and nanotechnology program of the Dutch Ministry of Economic Affairs, Agriculture and Innovation (EL&I) and 130 partners.

*renema@physics.leidenuniv.nl

[1] G. N. Goltsman, O. Okunev, G. Chulkova, A. Lipatov, A. Semenov, K. Smirnov, B. Voronov, A. Dzardarov, C. Williams, and R. Sobolewski, *Appl. Phys. Lett.* **79**, 705 (2001).

- [2] M. Eisaman, J. Fan, A. Migdall, and S. Polyakov, *Rev. Sci. Instrum.* **82**, 071101 (2011).
- [3] F. Marsili, V. B. Verma, J. A. Stern, S. Harrington, A. E. Lita, T. Gerrits, I. Vayshenker, and B. Baek, *Nat. Photonics* **7**, 210 (2013).
- [4] A. Semenov, A. Engel, H.-W. Hübers, K. Ilin, and M. Siegel, *Eur. Phys. J. B* **47**, 495 (2005).
- [5] A. N. Zotova and D. Y. Vodolazov, *Phys. Rev. B* **85**, 024509 (2012).
- [6] L. N. Bulaevskii, M. J. Graf, C. D. Batista, and V. G. Kogan, *Phys. Rev. B* **83**, 144526 (2011).
- [7] L. N. Bulaevskii, M. J. Graf, and V. G. Kogan, *Phys. Rev. B* **85**, 014505 (2012).
- [8] A. Engel, K. Inderbitzin, A. Schilling, R. Lusche, A. Semenov, D. Henrich, M. Hofherr, K. Il, and M. Siegel, *IEEE Trans. Appl. Supercond.* **23**, 2300505 (2013).
- [9] A. Gurevich and V. M. Vinokur, *Phys. Rev. Lett.* **100**, 227007 (2008).
- [10] A. Gurevich and V. M. Vinokur, *Phys. Rev. B* **86**, 026501 (2012).
- [11] D. Y. Vodolazov, *Phys. Rev. B* **85**, 174507 (2012).
- [12] M. Hofherr, D. Rall, K. Ilin, M. Siegel, A. Semenov, H.-W. Hübers, and N. A. Gippius, *J. Appl. Phys.* **108**, 014507 (2010).
- [13] R. Lusche, A. Semenov, H.-W. Huebers, K. Ilin, M. Siegel, Y. Korneeva, A. Trifonov, A. Korneev, G. Goltsman, and D. Vodolazov, *IEEE Trans. Appl. Supercond.* **23**, 2200205 (2013).
- [14] K. Suzuki, S. Shiki, M. Ukibe, M. Koike, S. Miki, Z. Wang, and M. Ohkubo, *Appl. Phys. Express* **4**, 083101 (2011).
- [15] A. D. Semenov and A. A. Korneev, *Physica (Amsterdam)* **351C**, 349 (2001).
- [16] A. D. Semenov, P. Haas, H.-W. Hübers, K. Ilin, M. Siegel, A. Kirste, T. Schurig, and A. Engel, *Physica (Amsterdam)* **468C**, 627 (2008).
- [17] A. Verevkin, J. Zhang, R. Sobolewski, A. Lipatov, O. Okunev, G. Chulkova, A. Korneev, K. Smirnov, G. N. Gol'tsman, and A. Semenov, *Appl. Phys. Lett.* **80**, 4687 (2002).
- [18] A. Verevkin *et al.*, *J. Mod. Opt.* **51**, 1447 (2004).
- [19] T. Yamashita, S. Miki, W. Qiu, M. Fujiwara, M. Sasaki, and Z. Wang, *Appl. Phys. Express* **3**, 102502 (2010).
- [20] H. Bartolf, A. Engel, A. Schilling, K. Ilin, M. Siegel, H.-W. Hübers, and A. Semenov, *Phys. Rev. B* **81**, 024502 (2010).
- [21] A. Korneev *et al.*, *Appl. Phys. Lett.* **84**, 5338 (2004).
- [22] A. Korneev *et al.*, *IEEE Trans. Appl. Supercond.* **15**, 571 (2005).
- [23] A. M. Kadin, M. Leung, and A. D. Smith, *Phys. Rev. Lett.* **65**, 3193 (1990).
- [24] D. Bitauld, F. Marsili, A. Gaggero, F. Mattioli, R. Leoni, S. Jahanmirinejad, F. Lévy, and A. Fiore, *Nano Lett.* **10**, 2977 (2010).
- [25] J. S. Lundeen, A. Feito, H. Coldenstrodt-Ronge, K. L. Pregnell, C. Silberhorn, T. C. Ralph, J. Eisert, M. B. Plenio, and I. A. Walmsley, *Nat. Phys.* **5**, 27 (2008).
- [26] H. B. Coldenstrodt-Ronge, J. S. Lundeen, K. L. Pregnell, A. Feito, B. J. Smith, W. Mauerer, C. Silberhorn, J. Eisert, M. B. Plenio, and I. A. Walmsley, *J. Mod. Opt.* **56**, 432 (2009).
- [27] G. Brida, L. Ciavarella, I. P. Degiovanni, M. Genovese, L. Lolli, G. Mingolla, F. Piacentini, M. Rajteri, E. Taralli, and M. G. A. Paris, *New J. Phys.* **14**, 085001 (2012).
- [28] J. J. Renema, G. Frucci, Z. Zhou, F. Mattioli, A. Gaggero, R. Leoni, M. J. A. d. Dood, A. Fiore, and M. P. van Exter, *Opt. Express* **20**, 2806 (2012).
- [29] See Supplemental Material at <http://link.aps.org/supplemental/10.1103/PhysRevLett.112.117604> for an extensive discussion of our experimental methods.
- [30] The code used to perform our modified detector tomography is available from the corresponding author.
- [31] See Supplemental Material at <http://link.aps.org/supplemental/10.1103/PhysRevLett.112.117604> for an extensive discussion of quantum detector tomography.
- [32] R. Lusche, A. Semenov, H. Huebers, K. Ilin, M. Siegel, Y. Korneeva, A. Trifonov, A. Korneev, G. Goltsman, and D. Vodolazov, [arXiv:1303.4546](https://arxiv.org/abs/1303.4546).
- [33] See Supplemental Material at <http://link.aps.org/supplemental/10.1103/PhysRevLett.112.117604> for the properties of our three samples.
- [34] For the vortex nucleation model, we have set $\gamma = 0$ in the terminology of [32] throughout. This is a reasonable approximation for our experimental situation.
- [35] K. Ilin, D. Rall, M. Siegel, A. Engel, A. Schilling, A. Semenov, and H. Huebers, *Physica (Amsterdam)* **470C**, 953 (2010).
- [36] K. Inderbitzin, A. Engel, and A. Schilling, *IEEE Trans. Appl. Supercond.* **23**, 2200505 (2013).
- [37] A. Engel and A. Schilling, *J. Appl. Phys.* **114**, 214501 (2013).